Slow compaction of granular systems

2005 J. Phys.: Condens. Matter 17 S2743

(http://iopscience.iop.org/0953-8984/17/24/024)

INSTITUTE OF PHYSICS PUBLISHING JOURNAL OF PHYSICS: CONDENSED MATTER

J. Phys.: Condens. Matter **17** (2005) S2743–S2754 doi:10.1088/0953-8984/17/24/024

Slow compaction of granular systems

P Ribière[1], P Philippe[2], P Richard[1], R Delannay[1] and D Bideau[1]

[1] Groupe Matière Condensée et Matériaux, UMR 6626, Université Rennes I, 35 042 Rennes Cedex, France
[2] Cemagref, Aix en Provence, Le Tholonet BP 31, 13 612 Aix-en-Provence Cedex 1, France

Received 16 March 2005
Published 3 June 2005
Online at stacks.iop.org/JPhysCM/17/S2743

Abstract

The dynamics of granular compaction under vertical tapping is experimentally and numerically studied for isotropic and anisotropic grains. It is shown that if convection takes place in the medium, it has a strong influence on the compaction dynamics. The local behaviour of the grains during compaction and the consequences for the global properties of the medium are investigated.

Introduction

Granular media are collections of discrete particles whose size is larger than some micrometres. This size leads to one of the most important characteristics of these systems: they are athermal, i.e. their gravitational energy is very large compared with the thermal energy $k_B T$. Another important characteristic is that they are dissipative: when grains are moving, they lose their kinetic energy quickly by inelastic collisions or friction. For example, when strongly agitated (shaken), an ensemble of grains appears to be similar to a gas, but it loses its energy very quickly, essentially by collisions. To maintain this gaseous state, an energy supply is consequently required.

It was outlined a long time ago that the static structures of dense disordered packings are similar to liquids or glasses [1]. But recently, this analogy has been used also for dynamic properties. It has been suggested in particular that the relaxation of a granular medium subjected to weak mechanical perturbations (tapping, shearing, ...) has a formal analogy with the slow dynamics of out-of-equilibrium thermal systems [2–4]. This analogy is based on the assumption that the geometry is the essential physical parameter of the system, and not the interactions between particles or the driving energy. Although mechanical agitation is neither stochastic nor isotropic, relaxation of granular media is often presented in this context as an ideal system for studying out-of-equilibrium dynamics.

The first experiments in this field were done in Chicago [5, 6]. Starting from a loose packing of beads confined in a narrow tube, a succession of vertical taps of controlled acceleration induces a progressive and very slow compaction of the system: after more than 10 000 taps, a steady state is still not reached. An empirical law in the inverse of the logarithm

of the number of taps (in other words, the time) was proposed to describe the evolution of the volume fraction:

$$\rho(t) = \rho_{\mathrm{f}} - \frac{\rho_0 - \rho_{\mathrm{f}}}{1 + B\ln(1 + t/\tau)}, \tag{1}$$

where ρ_{f} (the packing fraction for $t \to \infty$), ρ_0 (the initial packing fraction), B and τ are adjustable parameters. These results have motivated many theoretical and numerical works, most of them dealing with the concept of free volume or geometrical constraint [7–9]. Some of them underscore structural ageing effects, as currently noticed in glassy systems.

Our group has performed experiments and numerical simulations on this subject for some years. We give here an account of most of the results we obtained. The first part of this paper is a description of the behaviour of global quantities, such as the packing fraction, in compaction experiments, followed by a discussion about the importance of convection in the slow relaxation. The second part accounts for experimental and numerical results at the microscopic scale.

1. Compaction and global mechanisms

1.1. Dynamics of compaction

Recently, we have carried out compaction experiments [10], in a geometrical configuration different from that used in Chicago. Our experimental set-up is larger: a glass cylinder of diameter $D \sim 10$ cm is filled to a height of about 10 cm with 1 mm beads. A reproducible method used to build the initial packing gives a packing fraction around 0.58. This geometrical configuration allows only negligible wall effects, contrary to the Chicago group's experimental case, but convection is observed. This container is placed on a plate which is subjected to vertical taps given by an electromagnetic exciter (LDS V406). Each tap is created by one entire period of sine wave at a fixed frequency $f = 30$ Hz. The resulting motion of the whole system, monitored by an accelerometer at the bottom of the container, is however more complicated than a simple sine wave. At first the system undergoes a positive acceleration followed by a negative peak with a minimum $-\gamma_{\max}$. This negative peak acceleration is used to characterize the tap intensity by the dimensionless acceleration $\Gamma = \gamma_{\max}\ \mathrm{g}^{-1}$. The interval between two consecutive taps is $\Delta t = 1$ s. The packing fraction is measured using a γ-ray absorption set-up which allows us to explore the packing fraction of the medium along the symmetry axis or on average. The relaxation laws obtained are different from those given by Knight *et al* [5], especially for the long time behaviour. A steady state is clearly established and the relaxation is better fitted by the Kohlrausch–Williams–Watts law (KWW law) [11], or stretched exponential:

$$\rho(t) = \rho_{\mathrm{f}} - (\rho_{\mathrm{f}} - \rho_0)\exp[-(t/\tau)^{\beta}] \tag{2}$$

where ρ_{f} and ρ_0 correspond respectively to the steady state and to the initial packing fraction value. The adjustable parameters τ and β are respectively the relaxation time and the stretching of the exponential. This characteristic timescale τ is found to be very well described by an Arrhenius behaviour:

$$\tau = \tau_0 \exp\left(\frac{\Gamma_0}{\Gamma}\right). \tag{3}$$

Such a relaxation law is also found for strong glasses. Here the dimensionless acceleration Γ plays the role of a temperature.

Another quantity of interest is the final packing fraction: ρ_{f}. For this important parameter too, there is a strong discrepancy between the Chicago results and ours. In the former case this packing fraction is found to increase with the tapping intensity Γ whereas it is found to

decrease in the latter (see [2]). These discrepancies are related to the fact that the Chicago experiments were performed on a region where the system is far from being stationary while our experiments are focusing on the stationary regime. This is likely to originate from the difference in confinement between the two experiments. Indeed, in the Chicago group's work, the strong boundary effects lead to order creation, at least close to the sidewalls, and to packing fractions higher than that of the random close packing $\rho = 0.64$. In contrast all the final packing fractions we obtained for glass beads and with a very low confinement are below this value. Nevertheless, unlike the results found in Chicago [5, 6], our results are affected by convection. Indeed, as reported in [10, 12], a significant change is observed in the dependence of ρ_f on Γ which might correspond to different convective regimes.

It should be pointed out that all the studies reviewed above deal with isotropic granular media. Of course, most actual granular materials are far from being isotropic and the grain shape may modify the behaviour of the system during compaction. Villarruel *et al* [13] have shown, using the Chicago set-up, that a nematic ordering can be observed for compaction of rods. We carried out experiments on compaction of rice with the set-up in Rennes (low confinement) [14]. The anisotropic grains used here were rices of different shapes: long grains (basmati rice) and round rice. In order to quantify the grain anisotropy, each grain is likened to an ellipsoid and the mean ratio between the two axes is measured. We obtained 2.5 for the basmati rice and 1.5 for the round rice. The method used to build our initial packing, already used for spheres, is reproducible and gives $\phi \approx 0.55$ for basmati rice and $\phi \approx 0.56$ for round rice.

Figure 1 shows the evolution of the packing fraction with the number of taps for the two kinds of rice and for $\Gamma = 2.4$ and 6.0. The first observations are that whereas final packing fractions for round rice are comparable to what is obtained for compaction of sphere packings, it can be much higher for the basmati rice and close to the values obtained for compaction of ellipsoids [15]. Nevertheless, unlike Villarruel *et al* [13], we do not observe an ordered phase in which the grains tend to align vertically; this order could be due to the strong lateral confinement in a system where the length of the rods used is the same as the diameter of the cylindrical container (i.e. the steric constraints are huge). The aspect ratio of the grains ($\approx$4 for the rods) is probably also an important parameter.

1.2. Importance of convection in the compaction mechanisms

In the cases of packings of spherical glass beads and of rice, a slow convective flow takes place in the medium. In the case of spheres, two different regimes are observed according to the value of Γ, with a crossover $\Gamma_c \approx 2$. This corresponds to a significant change in the dependence of ρ_f on Γ. Above Γ_c, the free surface heaps up moderately and finally takes on a flat conical shape; this is probably brought about by a nearly toroidal convection roll which is the expected form of the convection flow in a cylinder with high enough acceleration [16]. Below Γ_c, the free surface progressively slopes along a preferred orientation which indicates a spontaneous breaking of the cylindrical symmetry on behalf of a plane symmetry (see figure 2).

The steady state slope of the inclined plane tends to increase when Γ decreases, but the time for this to happen becomes extremely long. These kinds of surface instabilities have been observed previously [17]. As shown in figure [2], the convective flow observed through the displacement of dyed tracers near the wall is asymmetrical with a fastest zone below the bottom of the inclined free surface.

The same experiments above Γ_c show a much less asymmetrical flow. We have checked that an unavoidable and very slight bias (less than a tenth of a degree) inherent to the set-up gives rise to an asymmetrical mass flow and to an inclination of the free surface which, at low

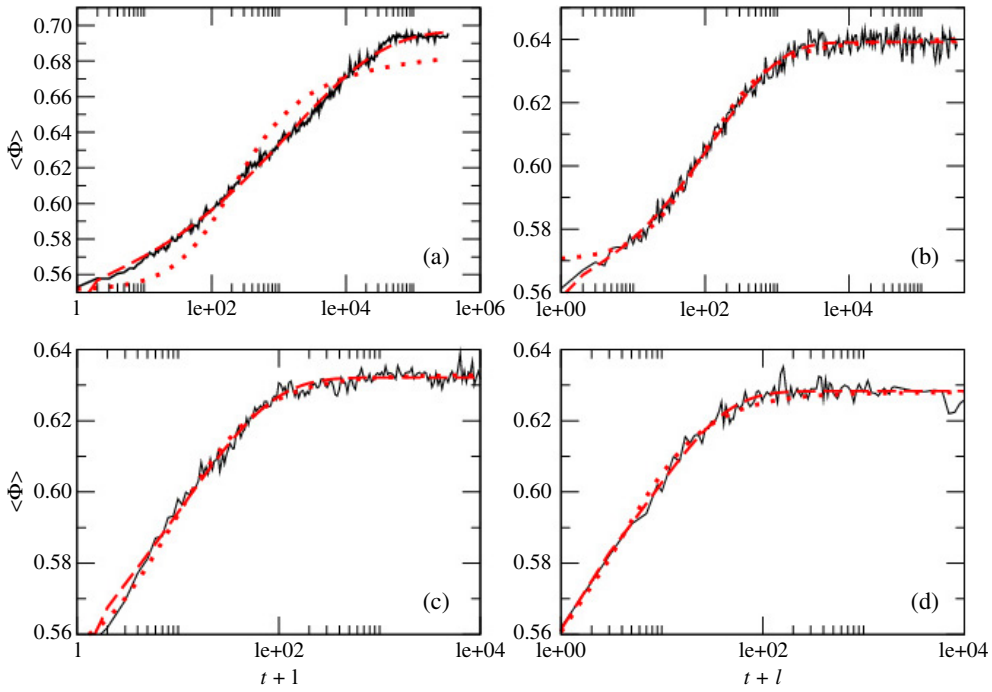

Figure 1. Evolution of the mean packing fraction of (a) basmati rice with $\Gamma = 2.4$, (b) round rice with $\Gamma = 2.4$, (c) basmati rice with $\Gamma = 6$ and (d) round rice with $\Gamma = 6$. The fit of the Chicago group (dotted line) and the fit of the KWW law (dashed line) are reported for each curve.

(This figure is in colour only in the electronic version)

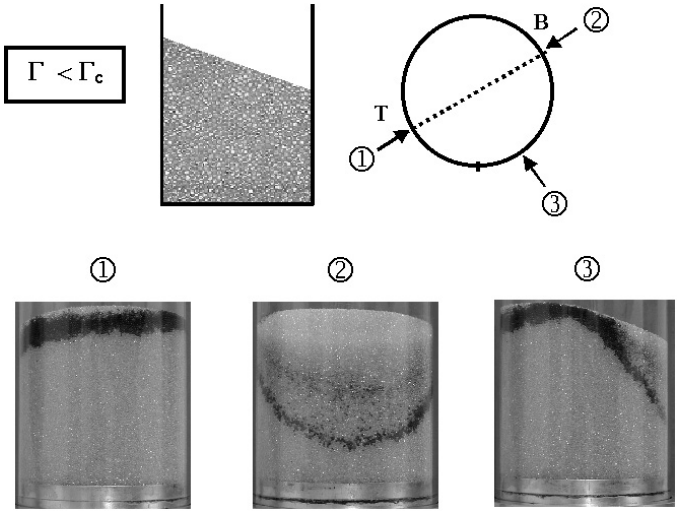

Figure 2. Convection at low accelerations. The drawings are the front view of the cylindrical container, with the free surface, and the top view, with the symmetrical plane shown as a dotted line (T and B denote the top and the bottom of the surface). The photographs correspond to three different views indicated on the upper drawing.

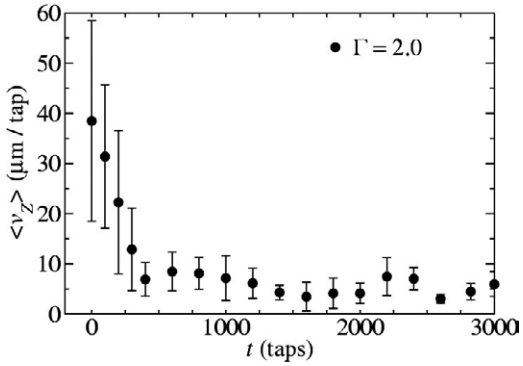

Figure 3. Convection intensity as a function of time. The system quickly reaches a steady state.

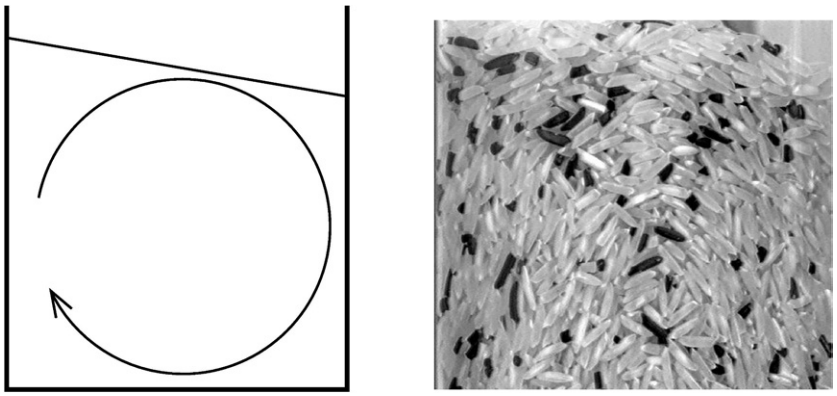

Figure 4. Sketch of the convection obtained for basmati rice and for $\Gamma = 6$ (left) and a snapshot of the media during relaxation (right) where convection roll can be clearly seen on the sidewalls.

acceleration and for long times, cannot be counterbalanced by any surface avalanche induced by the taps. We have measured the convection intensity through the displacement of a ring of dyed tracers initially placed at the periphery of the free surface. The downward velocity near the wall is deduced from the maximum cumulative displacement of the tracers. It progressively decreases as the packing compacts and finally reaches a steady state value, as can be seen in figure 3.

With anisotropic grains, the convection is more spectacular. As for spheres, depending on the value of Γ, two kinds of phenomena can be observed for basmati rice. For high values of Γ, convection is observed in the whole medium, whereas for low values of Γ, convection is localized in the upper part of the packing and is not steady. For $\Gamma > 3$, the convection takes place quickly in the medium and convection rolls are observed at the container wall (see figure 4). It should be pointed out that we only consider values of Γ larger than the lift-off threshold [10].

Using regular acquisition of images after each mechanical perturbation, we can measure a characteristic time τ_{conv} for the evolution of the convection rolls. For basmati rice subjected to taps of intensity $\Gamma = 6$, $\tau_{\mathrm{conv}} = 50$. The best KWW fit of the compaction law (equation (2)) gives $\tau = 30$, comparable to τ_{conv}. The same thing is observed for all experiments with $\Gamma > 3$.

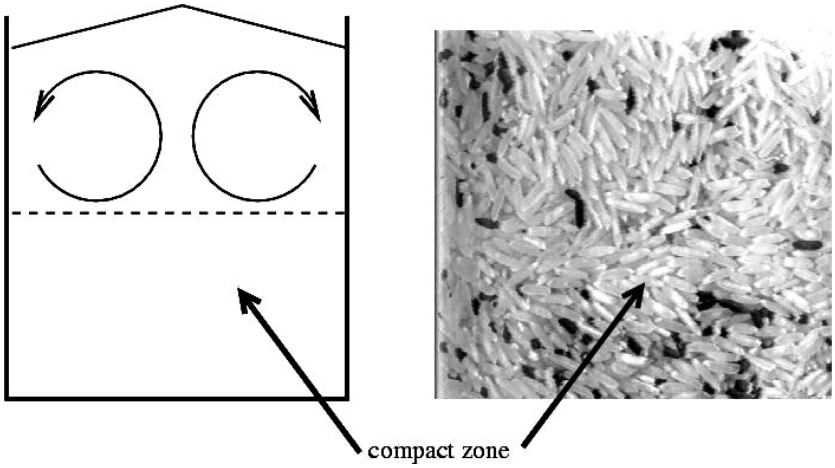

Figure 5. Sketch of the convection obtained for basmati rice and for $\Gamma = 2.4$ (left) and a snapshot of the media during relaxation (right) where the compact and ordered part can be clearly seen on the sidewalls.

A completely different behaviour is observed with $\Gamma < 3$. After a transient regime, the convection is extremely slowed down by compaction. For basmati rice and for a tapping strength of $\Gamma = 2.4$, the convection is totally stopped in most of the packing after $t \sim 1500$. Convection rolls do not exist any longer, except near the free surface (see figure 5). An interesting point is the following: the convection rolls compact the lowest part of the packing and tend to align the grains horizontally. Note that this order is different to the one observed by Villaruel *et al* [13]. Two parameters are probably crucial for the appearance of order: the gap between the sidewalls of the vessel and the aspect ratio of the grains.

It is possible to reach a better understanding of the observed phenomena by using a high speed camera (1000 images s^{-1}) to analyse the grain motion during a tap. Four phases can be distinguished:

- The rice follows the motion of the plate (phase 1).
- The rice takes off from the bottom (phase 2).
- The rice lands on the bottom (phase 3).
- A compression wave propagates throughout the medium (phase 4).

The rate of compaction and dilatation can be measured during these different phases. We have shown (see [14] for details) that the compression wave observed during the fourth phase corresponds to a significant compaction of the medium. So, in our set-up, convection and compaction are strongly linked. The compression wave is a consequence of the dissipation of the interaction energy stored by the grains during the first three phases of the motion. This allows the grains to move slightly around their initial position and to find a more stable position corresponding to a higher value of the packing fraction.

2. Behaviour at the microscopic scale

The above description is restricted to the (global) macroscopic scale. In this section, we present studies at the microscopic scale: the first one is carried out as x-ray microtomography experiments and the second one is a numerical simulation of the motion of grains during the compaction process.

X-ray tomography provides measurements of the 3D structure of mesoscale materials. Applied to granular matter, it allows one to access to the position of the grains. We recently used this technique to study the position of grains during granular compaction. The x-ray microtomography set-up is provided by the ESRF (European Synchrotron Radiation Facilities) ID19 beamline. A monochromatic coherent beam is used to get sample radiography for 1200 angular sample positions ranging from 0° to 180°. An x-ray energy of 51 keV has been selected to ensure a high enough signal-to-noise ratio. The exposure time is 1 s by projection and the energy is selected using a classical double-monocrystal device. A filtered back-projection algorithm is used to compute the three-dimensional mapping of the linear absorption coefficient in the sample. The light detector used is based on the FRELON CCD camera developed by the ESRF Detector group. The CCD array is made of 1024 by 1024 elements and is 14 bits dynamic. A thin scintillation layer deposited on glass converts x-rays to visible light. Light optics magnify the image of the scintillator and project it onto the CCD. With such a set-up we obtain a resolution of 9.81 μm by pixel. X-ray microtomography then allows one to have a fine and precise 3D reconstruction of the packing.

We use a set-up close to previous ones [18]: 200–400 μm diameter glass beads are poured up to about 80 mm height into a 8 mm inner diameter glass cylinder. Note that due to experimental limitations (beam size) the use of such a small system is necessary. The whole system is vertically shaken by sinusoidal excitation at a frequency of 70 Hz. The applied acceleration is measured by an accelerometer and the intensity of the vibration is characterized by Γ. The experiments are carried out as follows: starting from an initial loose reproducible configuration ($\phi \approx 0.57$) a packing is vibrated for a given number N of oscillations with a fixed acceleration Γ and then analysed by x-ray microtomography. Each reconstructed packing contains about 15 000 grains. Then, using image processing software, the size and location of each grain can be recovered.

Due to the long time needed to perform a three-dimensional mapping (about 1 h) and due to the large number of perturbations, the study of grain positions during each step of the compaction is unfortunately impossible. Nevertheless such a technique allows one to compare the packing microstructures at different stages of the compaction.

Figure 6 represents the variation of the pair correlation function $g(r)$ for the initial packing and after more than 10^4 excitations of intensity $\Gamma = 3$. Although the packing fraction increases during this compaction (from 0.57 to 0.62), no significant sign of this compaction is seen in $g(r)$. This is even true for steady state packings at different excitation intensities [18]. The function $g(r)$ appears to be an unsuitable tool for studying compaction.

Further evidence of a transformation in the packing microstructure can be provided by the size distribution of the interstitial voids. Moreover this can be an experimental test for the free volume theory that postulates an exponential decay for this size distribution:

$$\rho(v) = \exp\left(-\frac{v}{v_0}\right). \tag{4}$$

Following the work of Philippe and Bideau [19], we define a pore size via the Voronoï tessellation. A Voronoï polyhedron around a sphere is the region of space in which all points are closer to this sphere than to any other sphere in the packing. The Voronoï network, which is the whole collection of the edges and of the vertices of the polyhedra, maps the pore space. The volume of a pore is then the size of a virtual sphere centred on the vertex and in contact with the four neighbouring spheres. The volume of this void sphere partially represents the volume of the whole void volume situated inside the corresponding tetrahedron. Since in our experiments the spheres are not perfectly monosized, we have adapted this method to a polydisperse packing, replacing the Voronoï tessellation by the so-called navigation map [18].

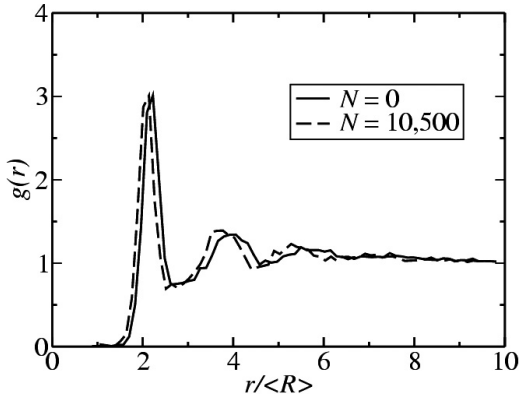

Figure 6. Evolution of the pair correlation function for $\Gamma = 3.0$.

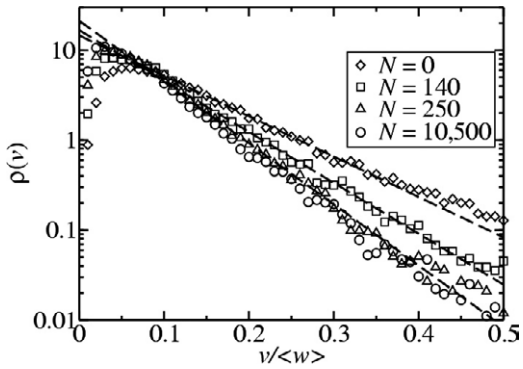

Figure 7. Evolution of the volume distribution of the pores during compaction with $\Gamma = 3.0$.

It is then possible to compute the size distribution of the pores for each packing. Following Philippe and Bideau [19] the volume of a pore v is normalized by the mean volume of the grains $\langle w \rangle$. Since previous theoretical works [20, 21] on a free volume model postulated an exponential decay (see equation (4)) for the distribution of the voids, we have reported our results on semi-log axes.

Figure 7 presents the evolution of the volume distribution of the pores for $\Gamma = 3.0$ at different stages of the compaction. First of all, we observe that, unlike the pair correlation function, $(\rho(v/\langle w \rangle)$ drastically changes with the number of excitations. An exponential decay law is found for the distribution of the voids, at least for the pores greater than octahedral pores $(v > \left(\sqrt{2} - 1\right)^3 \approx 0.0711)$. The exponential shape persists during the compaction of the packing, yet with a reduction of the tail, i.e. with a decrease of the characteristic volume v_0.

As reported in figure 8, the final exponential decays of the steady state distribution, obtained after a sufficient number of oscillations, are strongly dependent on the intensity Γ of the taps. By contrast, the part of the distribution corresponding to the smallest pores is less Γ dependent. The remarkable point is that these results are very close to those obtained by numerical simulations which are solely based on geometrical constraints in a three-dimensional packing of identical hard spheres [19].

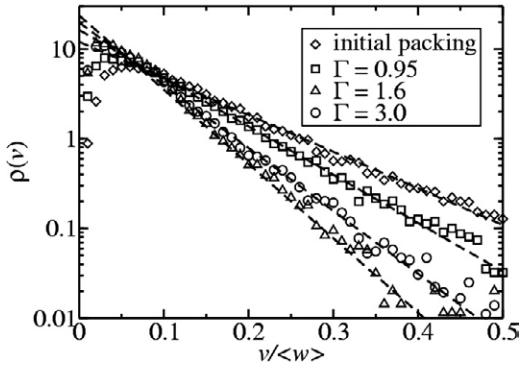

Figure 8. Evolution of the volume distribution of the pores for the initial packing and for three different steady state packings obtained for $\Gamma = 0.95$, 1.6 and 3.

The evolution of the void volume distribution is the consequence of the motion of individual grains. This motion has been studied using confocal microscopy in colloidal hard sphere suspensions [22] or in shear induced compaction of spheres [23]. These authors have found that the grain motion is not diffusive at the large scale and exhibits transient cage effects, similar to the one observed in glasses.

We have done the same type of study on our tapped sphere packings, both experimentally and numerically. The numerical model, close to that of the work of Barker and Metha [24], only takes into account the geometrical constraints [19]. In the simulation, the behaviour of 4096 spheres of radius R under consecutive taps is studied in a box of length $32R$ with lateral periodic boundary conditions, a flat bottom at $Z = 0$ and a free interface at the top of the packing. A tap is simulated in two stages. First the packing is dilated according to the law $(z - R) \rightarrow (z - R)\,(1 + \varepsilon)$ to increase the free volume and to allow the reorganization of the beads. This linear behaviour during a tap is observed in the experiment too and consequently the parameter ε can be directly linked to the experimental parameter Γ by a simple energetic analysis of the motion of the beads. The vertical displacement ΔZ can be written as

$$\Delta Z = \frac{0.5ma^2\omega^2}{mg} = \frac{\Gamma^2 g}{2\omega^2} \tag{5}$$

where a and w are respectively the amplitude and pulsation of the tap. So the dilation ε is proportional to Γ^2. The layer at the bottom is not allowed to move, in order to maintain a disordered layer and to avoid crystallization. The second stage simulates the gravitational redeposition of the spheres, with a non-sequential algorithm in order to observe collective behaviour. The complex succession of collisions of a bead is a sum of small motions obtained from a Monte Carlo algorithm. A displacement of length d and direction (θ, α) is tested on a randomly chosen bead. If this displacement does not create interpenetration with other beads, it is accepted. d is chosen randomly in the interval $[0; d_{\max}]$ with $d_{\max} = R/10$, θ is chosen above $(-\vec{u}_Z)$ using the Gaussian distribution

$$P(\theta) = A \exp\left(-\left(\frac{\theta}{\theta_0}\right)^2\right) \tag{6}$$

to simulate the effect of gravity and finally α is chosen randomly in $[0, \pi]$. The accuracy of the parameters is discussed in detail in [19]. The end of the tap is reached when all the last 4096 accepted motions are less than an arbitrary threshold (10^{-6}). This means that there is a small uncertainty on all the bead positions.

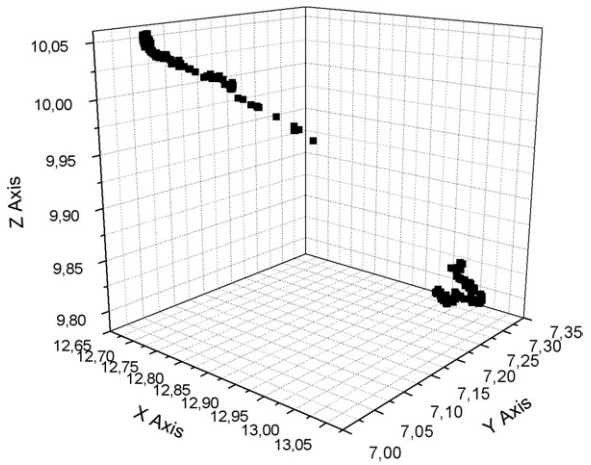

Figure 9. Displacement of a grain during the simulation. Extreme events (or jumps) can be observed.

Figure 9 shows the motion of a bead during a simulation. Its position during 100 taps from the initial state is given. After 46 'taps', the bead is subjected to a large jump: its displacement is 0.48, to be compared to the bead radius 0.5, when the average of the other displacements is about 0.0038 (i.e. they correspond to small motions in a cage). This result is quantitatively comparable to the one obtained by Pouliquen *et al* [23]. It is also comparable with the results obtained in our experimental work in progress using index matching technique.

To understand the importance of the jump for the evolution of the packing fraction, it is possible in the simulation to forbid this kind of motion, and then to compare the two evolutions, with and without 'jumps'. To forbid these large jumps, a test is added to the algorithm. After the non-interpenetration test, the program calculates d_i the displacement of the bead from the position before the dilatation. If the Z-displacement is negative, i.e. the bead is lower than initially, and if the displacement is bigger than twice the mean displacement of the beads in the same layer, the displacement is not always accepted, even if it does not interpenetrate the other elements, but it is accepted with an exponential probability $\exp\left(-\frac{(d_i-2\langle d\rangle)}{\delta}\right)$ where $\langle\cdot\rangle$ stands for the average on a layer, and δ is calculated in order to have the probability 10^{-5} when d_i is equal to the radius of the sphere. Preliminary results show that without jumps the compaction is slower. But what is more surprising is that the steady state reached by the packing fraction is less stable without a jump than with jumps. This means that high potential barriers, in terms of the energy landscape, separate the two states. Even if the 'jumps' are events of low probability, about 100 jumps during the 10 000 taps of the 4096 bead packings, they play an essential role for the evolution of the medium, and its reorganization.

3. Conclusion

In this paper, we have reported some experimental and numerical results concerning slow relaxation in granular media. Both the global evolution of the packing and the microscopic behaviour of the grains have been investigated.

Many questions remain open, especially concerning the correlation between the macroscopic behaviour of the medium and the grain motions. As reported in [25], granular media display strong ageing and memory effects. How can these phenomena be explained from

a microscopic point of view? It seems that the extreme events reported above (the jumps) play an important role in such phenomena, but how exactly? These questions are very challenging both from an experimental and from a numerical point of view. Another important question concerns the validity of a thermodynamic-like approach to granular matter and in particular the notion of temperature (see for example the paper of Baldassarri *et al* [26]). In other words, can we define a temperature (for example Edwards' temperature or a temperature defined via the fluctuation-dissipation theorem) and, if this temperature exists, what of its physical meaning? Most of the work on this subject deals with theoretical or numerical studies and very few experiments have been carried out. This is mainly due to the experimental determination of such a temperature being very difficult. Thus it is important to develop the experimental research further on this point.

Acknowledgments

We are indebted to Stéphane Bourlès and Patrick Chasle for technical support. We acknowledge the European Synchrotron Radiation Facility (ESRF) for the use of their facilities, hospitality and financial help. We thank Stéphane Bourlès, Xavier Thibault and Fabrice Barbe for their contribution to the experiments carried out at the ESRF. This work was supported by the ACI 'Energie et conception durable' of the French Ministry of Education and Research and by CNRS.

References

[1] Bernal J D 1964 *Proc. R. Soc.* A **280** 299
Sadoc J F 1981 *C. R. Acad. Sci., Paris* **292** 435
[2] Richard P, Nicodemi M, Delannay R, Ribière P and Bideau D 2005 *Nat. Mater.* **4** 121–8
[3] Edwards S F and Oakeshott R B S 1989 *Physica* A **157** 1080
Mehta A and Edwards S F 1989 *Physica* A **157** 1091
[4] Nicodemi M, Coniglio A and Herrmann H J 1997 *Phys. Rev.* E **55** 3962
Kurchan J 2000 *J. Phys.: Condens. Matter* **12** 6611
Liu A J and Nagel S R 1998 *Nature* **396** 21
[5] Knight J B, Fandrich C G, Lau C N, Jaeger H M and Nagel S R 1995 *Phys. Rev.* E **51** 3957
[6] Nowak E R, Knight J B, Ben-Aïm E, Jaeger H M and Nagel S R 1998 *Phys. Rev.* E **57** 1971
[7] Coniglio A and Nicodemi M 2001 *Physica* A **296** 451
Fierro A, Nicodemi M and Coniglio A 2002 *Europhys. Lett.* **59** 642
[8] Tarjus G and Viot P 2004 *Phys. Rev.* E **69** 11307
[9] Barrat A, Kurchan J, Loreto V and Sellito M 2000 *Phys. Rev. Lett.* **85** 5034
Colizza V, Barrat A and Loreto V 2002 *Phys. Rev.* E **65** 50301
[10] Philippe P and Bideau D 2003 *Phys. Rev. Lett.* **91** 104302
[11] Kohlrausch R 1854 *Pogg. Ann. Phys. Chem.* **91** 179
Williams G and Watts D C 1970 *Trans. Faraday Soc.* **66** 80
[12] Philippe P and Bideau D 2002 *Europhys. Lett.* **60** 677
[13] Villarruel F X, Lauderdale B E, Mueth D M and Jaeger H M 2000 *Phys. Rev.* E **61** 6914
[14] Ribière P, Richard P, Delannay R and Bideau D 2005 *Phys. Rev.* E **71** 011304
[15] Donev A, Cisse I, Sachs D, Variano E A, Stillinger F H, Connelly R, Torquato S and Chaikin P M 2004 *Science* **303** 990–3
[16] Evesque P and Rajchenbach J 1989 *Phys. Rev. Lett.* **62** 44
[17] Knight J B, Ehrichs E E, Kuperman V Y, Flint J K, Jaeger H M and Nagel S 1996 *Phys. Rev.* E **54** 5726
[18] Richard P, Philippe P, Barbe F, Bourlès S, Thibault X and Bideau D 2003 *Phys. Rev.* E **68** 20301
[19] Philippe P and Bideau D 2001 *Phys. Rev.* E **63** 51304
[20] Boutreux T and de Gennes P G 1997 *Physica* A **244** 59
[21] Caglioti E, Loreto V, Herrmann H J and Nicodemi M 1997 *Phys. Rev. Lett.* **79** 1575
[22] Weeks E R, Crocker J C, Levitt A C, Schofield A and Weitz D A 2000 *Science* **287** 627
Weeks E R and Weitz D A 2002 *Phys. Rev. Lett.* **89** 95704

[23] Pouliquen O, Belzons M and Nicolas M 2003 *Phys. Rev. Lett.* **91** 14301
[24] Barker G C and Mehta A 1992 *Phys. Rev.* A **45** 3435
Barker G C and Mehta A 1993 *Phys. Rev.* E **47** 184
[25] Josserand C, Tkachenko A V, Mueth D M and Jaeger H M 2000 *Phys. Rev. Lett.* **85** 3632
[26] Baldassarri A *et al* 2005 *J. Phys.: Condens. Matter* **17** S2405